Journal of Cluster Science (2024) 35:1601–1611
https://doi.org/10.1007/s10876-024-02595-z

ORIGINAL PAPER

$[Mo_2O_2S_2]$-Based Oxothiomolybdates and Their Reactivity with Pyrazole and Triazole

Anna V. Konkova[1] · Darya V. Evtushok[1] · Natalia V. Kuratieva[1] · Anton A. Ivanov[1] · Michael A. Shestopalov[1]

Received: 4 December 2023 / Accepted: 19 February 2024 / Published online: 13 April 2024

Abstract

Extending the family of oxothiomolybdates, the interaction of the cyclic anion $[Mo_8O_8S_8(OH)_8(C_2O_4)]^{2-}$ and the complex $[Mo_4O_4S_4(C_2O_4)_5]^{6-}$ with organic compounds of the azole series—pyrazole (pzH) and 1,2,4-triazole (trzH) in water solution and in the melt of ligands was investigated. In water solution pyrazole plays only the role of cation (upon protonation) to form the complex $(pzH_2)_2[Mo_2O_2S_2(C_2O_4)_2(H_2O)_2]$. While in the reaction in melt of pzH in the case of the initial cyclic anion, the resulting anionic product $[Mo_6O_6S_6(pz)_6(MoO_4)]^{2-}$ represents a pioneering example of a cyclic oxothiometalate $\{Mo_6\}$ anchored by the coordination of six bridging pyrazolates (pz), complemented by a MoO_4^{2-} core. At the same time, the interaction of $[Mo_4O_4S_4(C_2O_4)_5]^{6-}$ with pzH and trzH melts yields the binuclear clusters $[Mo_2O_2S_2(C_2O_4)_2L_2]^{2-}$, where L = pzH or trzH. The composition and structures of the compounds were determined using a variety of physicochemical methods, including single-crystal X-ray diffraction analysis.

Keywords Oxothiomolybdate · Cluster · Crystal structure · Pyrazole · Triazole

Introduction

Polyoxothiometalates—a distinct subclass of polyoxometalates characterizing by the partial replacement of oxygen atoms with sulfur, are of great interest due to diverse structural features and promising catalytic properties [1]. One of the most common representatives of this class in the literature are binuclear clusters containing the $\{Mo^V_2O_2(\mu-S)_2\}^{2+}$ fragment. Due to redox properties and ability to coordinate both organic and inorganic ligands, this fragment serves as a central structural motif in the synthesis of cyclic oxothiometalates, represented as $[(Mo_2O_2S_2(OH)_2)_nL_m]^{q-}$ (where n ranges from 3 to 10, m from 1 to 4, depending on the ligand L, and q denotes the charge) [2–5]. The formation of these cyclic entities is the result of the self-condensation of $[Mo_2O_2S_2]^{2+}$ fragments in an aqueous medium with a pH between 5 and 7 under the control of a ligand L, which determines the size of the cycle [6]. Carboxylic acids, either with rigid or flexible backbones, are mainly used as ligand-templates [5, 6]. Such compounds have been shown to be promising catalytic systems, including in hydrogen evolution reactions [7, 8].

In addition to the compounds described above, a number of complexes of binuclear clusters $\{Mo_2O_2S_2\}$ with various organic ligands have been reported in the literature: (i) amino acids such as glycine, cysteine and histidine [9–14]; (ii) EDTA derivatives or nitrilotriacetate [9, 11, 15–17]; (iii) thiosemicarbazone and its derivatives [18, 19]; (iv) pyridine and its derivatives [20–23]. In addition to their catalytic properties, such compounds have shown promise in biology and medicine as antiviral, antibacterial and anticancer agents [18, 19].

Extending this class of compounds, in this work N-donor heterocyclic compounds, pyrazole (pzH) and 1,2,4-triazole (trzH), have been chosen as organic ligands for the formation of new complexes. In addition to the presence of a coordination center (nitrogen atom in the second position), this type of ligands exhibits acid-base properties and contains two nitrogen atoms in adjacent positions, due to which they can act as bridging ligands, promoting the formation of new unusual compounds. On the other hand, such biologically active ligands [24, 25] can expand the practical applications of oxothiomolybdates.

The starting compounds chosen in this work were $[Mo_8O_8S_8(OH)_8(C_2O_4)]^{2-}$ (denoted as **(1)**) and

✉ Darya V. Evtushok
evtushok@niic.nsc.ru

[1] Nikolaev Institute of Inorganic Chemistry SB RAS, 3 Acad. Lavrentiev Ave., 630090 Novosibirsk, Russia

$[Mo_4O_4S_4(C_2O_4)_5]^{6-}$ (denoted as **(2)**). Despite the methods described in the literature for obtaining these complexes, their synthesis was optimized so that it was possible to obtain these complexes in high yields (for example 80% versus the literature 20% for **(1)**) in a short time (several hours instead of a weeks). The work then demonstrated the interaction of these compounds with pyrazole and triazole under different conditions. During the studies, it was shown that reactions in the melt of an organic ligand led to the formation of either $[Mo^V_6O_6S_6(pz)_6(Mo^{VI}O_4)]^{2-}$ or dinuclear clusters $[Mo^V_2O_2S_2(C_2O_4)_2L_2]^{2-}$ (L = pzH, trzH), depending on the structure of the initial oxothiomolybdate. The formation of a particular compound has been confirmed by a number of physicochemical methods, including single crystal X-ray diffraction analysis.

Experimental Part

Materials and Methods

$K_{2-x}(Me_4N)_x[I_2Mo_{10}O_{10}S_{10}(OH)_{10}(H_2O)_5]$ (0 < x < 0.5) was synthesized according to reported procedure [26, 27]. All other reactants and solvents were purchased and used as received.

Elemental analyses were obtained using a vario MICRO cube analyzer and EuroVector EA3000. Energy-dispersive X-ray spectroscopy (EDS) was performed on a Hitachi TM3000 TableTop SEM with Bruker QUANTAX 70 EDS equipment. FTIR spectra were recorded on a Bruker Vertex 80 as KBr disks. The thermal properties (TGA) were studied on a Thermo Microbalance TG 209 F1 Iris (NETZSCH) from 25 to 800 °C at the heating rate of 10 °C·min^{-1} in He flow (30 mL·min^{-1}). Powder X-ray diffraction patterns were collected on a Philips PW 1820/1710 diffractometer (CuK_α radiation, graphite monochromator and Si as an external reference).

The ^{1}H NMR spectra of sample were obtained from D_2O or DMSO-d_6 solution at room temperature on a Bruker Avance 500 spectrometer with working frequency of 499.93 MHz for ^{1}H. The ^{1}H chemical shifts are reported in ppm of the δ scale and referred to the signal of the solvents (δ = 2.50 or 4.76 ppm for residual protons of DMSO-d_6 or D_2O correspondingly).

Synthetic Procedures

Synthesis of $K(Me_4N)[Mo^V_8O_8S_8(OH)_8(C_2O_4)]\cdot 7H_2O$ (Denoted as (1))

A suspension of $K_{2-x}(Me_4N)_x[I_2Mo_{10}O_{10}S_{10}(OH)_{10}(H_2O)_5]$ (0.5 g, 0.24 mmol) was prepared in 10 mL of distilled water at room temperature. Then, 10 mL of a 0.8 M oxalic acid (8 mmol) water solution was added, after which the color of the reaction mixture changed from yellow to red. After stirring for 30 min, the mixture was filtered to obtain a red filtrate. The pH of this filtrate was then adjusted to 7 by slowly adding of 4 M potassium hydroxide aqueous solution drop by drop while stirring. The desired product precipitates from the reaction mixture as a yellow crystalline powder. The neutralization procedure takes approximately 10 min. The precipitate is separated by centrifugation and washed sequentially with water (10 mL), ethanol (20 mL) and diethyl ether (20 mL). Yield: 391 mg (80% based on the starting molybdenum cluster). For $C_6H_{34}KMo_8NO_{27}S_8$ calcd: C 4.5; H 2.1; N 0.9; S 15.9. Found: C 4.0; H 2.4; N 0.8; S 16.3. EDS: K: Mo: S ratio of 1.2: 8.0: 7.7. IR (KBr, cm^{-1}) is shown in Fig. S1. The TGA revealed a weight loss of ~ 7.5% from 40 to 130 °C (the calculated weight loss of 7 H_2O is 7.8%) (Fig. S2). Crystals of $(Me_4N)_2[Mo_8O_8S_8(OH)_8(C_2O_4)]\cdot 5.45DMF\cdot 2.55Me_2CO\cdot 0.5H_2O$ (denoted as **(1a)**) were obtained by slow vapor diffusion of acetone in N,N-dimethylformamide (DMF) solution of **(1)**.

Synthesis of $K_6[Mo^V_4O_4S_4(C_2O_4)_5]\cdot 9H_2O$ (Denoted as (2))

The synthesis method of **(2)** is similar to **(1)**. However, the pH of the red filtrate was adjusted to 5 using a 4 M potassium hydroxide aqueous solution. After keeping the solution at +5°C for 2 days, red crystals of $K_6[Mo_4O_4S_4(C_2O_4)_5]\cdot 10H_2O$ (denoted as **(2a)**) are formed, which lose one molecule of water when dried in air resulting in **(2)**. Yield: 424 mg (50% based on starting molybdenum cluster). For $C_{10}H_{20}K_6Mo_4O_{34}S_4$ calcd: C 8.5; H 1.3; S 9.1. Found: C 8.5; H 1.5; S 8.6. EDS: K: Mo: S ratio of 5.4: 4.0: 3.9. IR (KBr, cm^{-1}) is shown in Fig. S1. The TGA revealed a weight loss of ~ 11.7% from 40 to 130 °C (the calculated weight loss of 9 H_2O is 11.5%) (Fig. S3).

Synthesis of $(pzH_2)_2[Mo_2O_2S_2(C_2O_4)_2(H_2O)_2]\cdot 3H_2O$ (Denoted as (3))

A suspension of $K_{2-x}(Me_4N)_x[I_2Mo_{10}O_{10}S_{10}(OH)_{10}(H_2O)_5]$ (0.25 g, 0.12 mmol) was prepared in 10 mL of distilled water at room temperature. Then, 10 mL of a 0.5 g oxalic acid (4 mmol) water solution was added, after which the color of the reaction mixture changed from yellow to red. After stirring for 30 min, the mixture was filtered to obtain a red filtrate with pH ∽ 1. Then 80 mg (1.2 mmol) of pyrazole were added under stirring to filtrate resulting in precipitation of product. The powder was washed with cold water, ethanol, diethyl ether and dried in air. Yield: 257 mg (61% based on starting molybdenum cluster). EDS: Mo: S ratio of 2.0: 2.3. Single crystals of the compound suitable for X-ray diffraction analysis were obtained from the filtrate (after removing of powder product) at 5 °C for several days. The TGA

revealed a weight loss of ~ 6.3% from 30 to 80 °C, which corresponds to 2.4H_2O. A weight loss of ~ 5.2% from 80 to 135 °C, which corresponds to 2H_2O (the calculated weight loss of 5H_2O is 13.0%) (Fig. S4).

Preparation of "$(Me_4N)_{2-x}K_x[Mo^V_6O_6S_6(pz)_6(Mo^{VI}O_4)]$·(Solvate)" (Denoted as (4))

Compound **(1)** (0.1 g, 0.06 mmol) and pyrazole (0.1 g, 1.47 mmol) were placed into a glass ampoule. The ampoule was sealed in an air environment and maintained at 140 °C for 48 h. Gradual cooling of the reaction mixture over 24 h resulted in the formation of orange and dark brown crystals. To remove excess pyrazole, the reaction mixture was washed 3 times with 20 mL diethyl ether. PXRD analysis indicated the presence of additional phases besides the target product. The impurities exhibited similar solubility characteristics to the target product, thus hindering the isolation of pure **(4)** and subsequent full characterization and yield determination. Single crystals of the $(Me_4N)_2[Mo_6O_6S_6(pz)_6(MoO_4)]$·2pzH (denoted as **(4a)**) suitable for X-ray diffraction analysis were obtained in melt of ligand after slow cooling of ampoule. The EDS for crystals separated from the reaction mixture: Mo: S: K ratio of 7.0: 6.3: 0.3.

Synthesis of $K_2[Mo^V_2O_2S_2(C_2O_4)_2(pzH)_2]$·0.5pzH·1.4$H_2O$ (Denoted as (5)) and $K_{1.5}H_{0.5}[Mo^V_2O_2S_2(C_2O_4)_2(trzH)_2]$·2trzH·$H_2O$ (Denoted as (6))

Compound **(2)** (0.1 g, 0.07 mmol) and the corresponding heterocycle (for pzH: 0.1 g, 1.47 mmol; for trzH: 0.1 g, 1.45 mmol) were placed in a glass ampoule. The ampoule was sealed in an air environment and maintained at 140 °C for 6 h. Slow cooling over 24 h led to the formation of red crystals for pzH and orange crystals for trzH. To remove the resulting impurities and excess of ligands, the crystals were washed 5 times with 5 mL ethanol with the addition of 200 µL of water, and with 5 mL of diethyl ether. Single crystals of the compounds suitable for X-ray diffraction analysis were obtained in melt of ligand after slow cooling of ampoule.

(5): Yield: 67 mg (68%). For $C_{11.5}H_{12.8}K_2Mo_2N_5O_{11.4}S_2$ calcd: C 18.7; H 1.7; N 9.5; S 8.7. Found: C 18.5; H 1.9; N 9.2; S 8.4. EDS: K: Mo: S ratio of 2.2: 2.0: 1.9. IR (KBr, cm^{-1}) is shown in Fig. S5. The TGA revealed a weight loss of ~7.8% from 35 to 140 °C (the calculated weight loss of 0.5pzH and 1.4H_2O is 8.0%) (Fig. S6).

(6): Yield: 70 mg (70%). For $C_{12}H_{14.5}K_{1.5}Mo_2N_{12}O_{11}S_2$ calcd: C 17.6; H 1.8; N 20.6; S 7.8. Found: C 17.5; H 2.1; N 20.8; S 7.3. EDS: K: Mo: S ratio of 1.7: 2: 2.2. IR (KBr, cm^{-1}) is shown in Fig. S7. The TGA revealed a weight loss of ~2.3% from 35 to 98 °C (the calculated weight loss of H_2O is 2.2%) (Fig. S8).

Crystallography

Single-crystal X-ray diffraction (SCXRD) data for **(1a)**, **(2a)**, **(3)**, **(4a)**, **(5)** and **(6)** were obtained at 150 K on a Bruker D8 Venture diffractometer with a CMOS PHOTON III detector and IµS 3.0 microfocus source (MoK_α radiation (λ = 0.71073 Å), collimating Montel mirrors). The crystal structures were solved using the SHELXT [28] and were refined using SHELXL [29] programs. All non-hydrogen atoms were refined anisotropically. Hydrogen atoms of solvate water and pyrazole molecules are not localized. Other refinement details are listed above.

(1a): The oxalate ligand ($C_2O_4^{2-}$) is disordered over two positions with SOF 0.673 and 0.327 or 0.598 and 0.402 for two independent cluster anions, which was refined by FVAR constraint. One DMF molecule disordered over two positions with SOF 0.59 and 0.41. One DMF molecule and one acetone molecule occupy the same volume with SOF 0.423 and 0.577 respectively. One NMe_4 is disordered over two positions with the slight shift of the molecule (SOF 0.611 and 0.389). The other NMe_4 is disordered by rotation around the N-C bond with SOF 0.567 and 0.433. The rest of the SOF constraints are related to the water or acetone disordering.

(4a): The central Mo–O fragment of the cluster anion is disordered over two positions (SOF 0.3 and 0.7). For two solvate pyrazole molecules have the disordering over two or four positions at the same place. Two methyl fragments of NMe_4 are disordered over two close positions with a ratio of 0.8:0.2.

(5): A K5 cation is disordered over two positions (SOF 0.871 and 0.129, refined using FVAR). The other SOF constraints concern the solvate water or pyrazole molecules disordered together or alone in the same position, with SOF varying from 0.125 to 0.75.

(6): Hydrogen atom of N-H of solvate 1,2,4-triazole molecule is disordered over two positions due to possible location on nitrogen atom at first or fourth position of triazole ring (SOF 0.64 and 0.36).

Table S1 summarizes crystallographic data, while CCDC 2299095, 2308359, 2308361-2308364 contain the supplementary crystallographic data for this paper. These data can be obtained free of charge from the Cambridge Crystallographic Data Centre via www.ccdc.cam.ac.uk/data_request/cif.

Results and Discussion

Synthesis, Structure and Characterization (1) and (2)

As mentioned in the introduction, complexes of different nuclearity are known for oxothiomolybdates with organic

acids. One of the representatives of such compounds is the anionic cyclic complex $[Mo^{V}_{8}O_8S_8(OH)_8(C_2O_4)]^{2-}$ ($[(Mo^{V}_{2}O_2(\mu-S)_2)_4(\mu-OH)_8(\mu_8-C_2O_4)]^{2-}$) (Fig. 1), which consists of four $\{Mo_2O_2S_2\}^{2+}$ fragments connected by bridging hydroxo ligands and an oxalate anion located in the cavity. Although the complex has been known since 2000, the synthesis methods described in the literature (original [4] and recently published [5]) have a number of difficulties and limitations. Both approaches involve the self-condensation of binuclear $\{Mo^{V}_{2}O_2S_2\}^{2+}$ clusters (formed by dissolving $K_{2-x}(Me_4N)_x[I_2Mo^{V}_{10}O_{10}S_{10}(OH)_{10}(H_2O)_5]$ in HCl) by adding oxalic acid and adjusting the pH of the solution to 4-5 with NaOH or KOH solution. The reaction products were isolated from the solution only by long-term crystallization (about 1 week). In the original work the yield was not reported, while in more recent work the product yield reached 20%.

In this work, the method for the synthesis of the anionic complex $[Mo^{V}_{8}O_8S_8(OH)_8(C_2O_4)]^{2-}$ was optimized in order to further study its reactivity with nitrogen heterocycles. $K_{2-x}(Me_4N)_x[I_2Mo^{V}_{10}O_{10}S_{10}(OH)_{10}(H_2O)_5]$ was also chosen as the starting compound, which was dissolved in a 0.8 M aqueous solution of oxalic acid (pH ∽ 1), i.e. the reaction was carried out without the use of hydrochloric acid. Slowly adjusting the pH of the solution to 7 using a 1 M solution of potassium hydroxide leads to the precipitation of the crystalline product $K(Me_4N)[Mo^{V}_{8}O_8S_8(OH)_8(C_2O_4)]\cdot 7H_2O$ (denoted as **(1)**) (Fig. 1) with a yield of 80%, the phase purity of which has been confirmed by X-ray powder diffraction analysis (Fig. S9), as well as by a complex of physicochemical analytical methods (see Experimental Part). As a result, we have reduced the time to obtain the compound from 1 week to about 1 h, and also significantly increased the yield of the target product. The use of potassium hydroxide instead of sodium hydroxide accelerates the precipitation of the compound and avoids long crystallizations. In addition, during the optimization of the synthesis method,

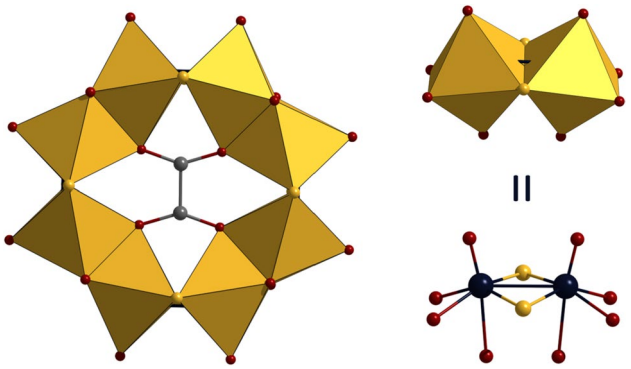

Fig. 1 Structure of cluster anion $[Mo^{V}_{8}O_8S_8(OH)_8(C_2O_4)]^{2-}$ in compound **(1)**. Color code: Mo—dark blue, S—yellow, O—red, C—gray, $Mo^{V}_{2}O_8S_2$—yellow edge-connected octahedrons (Color figure online)

reactions similar to those published (using HCl to dissolve $K_{2-x}(Me_4N)_x[I_2Mo^{V}_{10}O_{10}S_{10}(OH)_{10}(H_2O)_5]$) were also carried out, followed by adjustment of the pH of the solution using KOH. In this case, the yield of the reaction product (precipitated complex) was significantly lower (not higher than 20%) and its powder diffraction pattern was not consistent with the compound **(1)**. We believe that the addition of HCl to these syntheses may lead to by-products with chlorine as a ligand or interfere with cluster condensation, resulting in a mixture of different products. Therefore, using only oxalic acid as both a ligand and a source of acidic medium allows us to obtain a desired product in high yields.

By keeping the reaction mixture at pH ∽ 7 (before the product precipitated) and at 5 °C for 2 days, crystals of the compound **(1)** suitable for single-crystal X-ray diffraction analysis were obtained. The structure of the compound is similar to that published in [5]. Compound **(1)** exhibits solubility in polar solvents, including water, DMF and DMSO. Slow diffusion of acetone vapor into a DMF solution of **(1)** results in the crystallization of the salt $(Me_4N)_2[Mo^{V}_{8}O_8S_8(OH)_8(C_2O_4)]\cdot 5.45DMF\cdot 2.55Me_2CO\cdot 0.5H_2O$ (denoted as **(1a)**). The EDS analysis of the resultant crystal confirmed the absence of potassium. In the structure, the cluster anions are significantly more distant from each other, surrounded by tetramethylammonium cations and solvate molecules of DMF, acetone, and water (Fig. S10), and connected to each other by an extensive network of hydrogen bonds. The preservation of the structure of the cyclic cluster indirectly confirms its stability in organic solutions.

Adding a solution of potassium hydroxide to the reaction mixture resulted in a color change from red to orange only at a pH close to 7. Therefore, we also decided to obtain other products at lower pH values. The sequential condensation of cluster complexes with increasing pH is mentioned in the literature: from the only chelate coordination of the oxalate anion to the binuclear cluster at pH 1, through binuclear clusters connected by a bridging oxalate ligand at pH 2–4, to the formation of the cyclic anion $[Mo^{V}_{8}O_8S_8(OH)_8(C_2O_4)]^{2-}$ [4, 30]. Keeping the reaction mixture at pH 5 at 5 °C for 2 days resulted in the formation of large red crystals of the compound $K_6[Mo^{V}_{4}O_4S_4(C_2O_4)_5]\cdot 10H_2O$ (denoted as **(2a)**) (yield ∽ 50%), suitable for SCXRD, in which two $[Mo^{V}_{2}O_2S_2(C_2O_4)_2]^{2-}$ fragments are connected by oxalate ligand ($[(Mo^{V}_{2}O_2(\mu-S)_2(\eta^2-C_2O_4)_2)_2(\mu_4-C_2O_4)]^{2-}$) (Fig. 2a). The synthesis of similar anions $[Mo^{V}_{4}O_4Q_4(C_2O_4)_5]^{6-}$ (Q = O, S) [31–35] is also mentioned in the literature, one of which has the same anion fragment $[Mo^{V}_{4}O_4S_4(C_2O_4)_5]^{6-}$ as in **(2)** and the cation is 1,3-propyldiammonium [33]. Unfortunately, most of this works are not readily available, making it difficult to compare synthetic approaches and compound yields. Nevertheless, the method demonstrated in this work allows us to isolate such a product in good yield. Compound $K_6[Mo^{V}_{4}O_4S_4(C_2O_4)_5]\cdot 9H_2O$

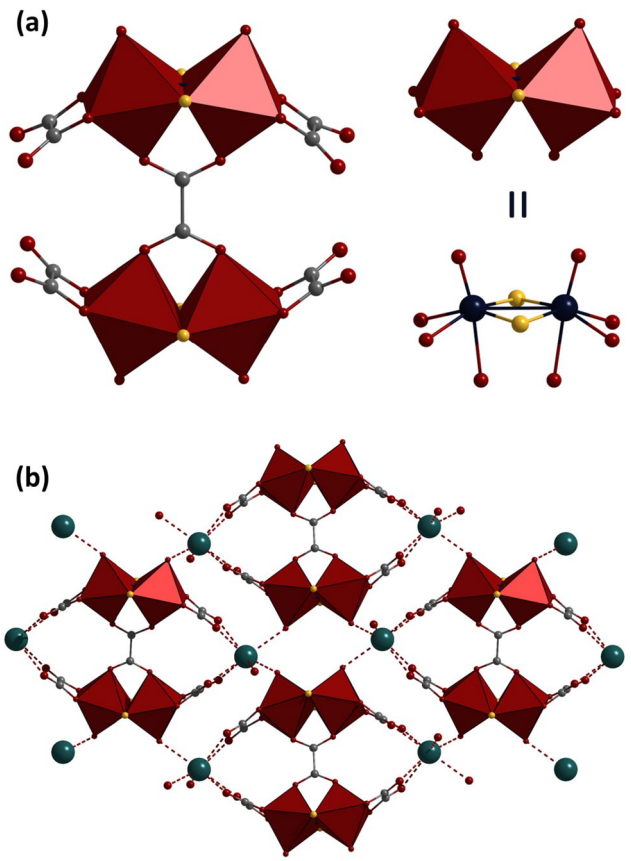

Fig. 2 Structure of cluster anion $[Mo^{V}_4O_4S_4(C_2O_4)_5]^{6-}$ (**a**) and packing of anions forming infinite layers (**b**) in crystal structure of compound (**2a**). Color code: Mo—dark blue, S—yellow, O—red, C—gray, K—dark cyan, $Mo^{V}_2O_8S_2$—red edge-connected octahedrons, K···O contacts—dashed red (Color figure online)

(denoted as (**2**)) (lose one water molecule upon drying) has been characterized by a number of physicochemical analytical methods. The powder X-ray diffraction pattern is in good agreement with the theoretical one (Fig. S11).

According to SCXRD, in (**2a**) cluster anions $[Mo^{V}_4O_4S_4(C_2O_4)_5]^{6-}$ are connected in infinite layers (Fig. 2b) by K···O contacts between potassium cations and oxygen atoms of oxalate ligands or oxo-ligands of $\{Mo^{V}_2O_2S_2\}^{2+}$ clusters (distances of 2.72–2.86 Å). The layers are connected to each other by other potassium cations through K···O contacts (distances of 2.88–3.07 Å). Solvate water molecules are either located in the free space between the layers or complement the coordination sphere of the potassium cations. The bond lengths of Mo–Mo, Mo = O, Mo–μ–S, Mo–O align with the literature values for $\{Mo^{V}_2O_2S_2\}^{2+}$ and are summarized in Table S2.[33] Comparison of the distances with other anions $[Mo^{V}_4O_4Q_4(C_2O_4)_5]^{6-}$ (Q = O, S) shows that substitution of the bridging sulfur ligands with oxygen results in a shortening of the Mo-Mo bond length from 2.824 to 2.666 Å. Conversely, the Mo–$O^{\mu-ox}$ bond associated with oxalate-bridged molybdenum fragments lengthens from 2.303 to 2.368 Å. No consistent trend is evident for the other bonds. In compounds (**1**) and (**2a**), the Mo–Mo and Mo–μ–S bonds are comparable. However, the Mo–$O^{\mu-ox}$ bonds in the cyclic compound (**1**) are slightly longer, namely 2.457–2.504 vs 2.308–2.320 Å in (**2a**) due to the adaptation to the cyclic structure.

It is important for further steps of this work (interaction with organic ligands) to study the stability of the resulting complexes at different temperatures. TGA and DTG curves were obtained in an argon atmosphere with a heating rate of 10 °C/min (Figs. S2, S3). In general, the thermal decomposition behavior of these compounds follows three steps: (i) removal of solvate molecules up to 130 °C; (ii) decomposition of oxalate ligands below 350 °C; (iii) decomposition of cluster fragments $\{Mo^{V}_2O_2S_2\}^{2+}$ up to 800 °C. Thus, in the first step both compounds lose all solvent water molecules with a weight loss of 7.5 and 11.7% for (**1**) and (**2**) respectively, which is in good agreement with the theoretical values (7.8 and 11.5%). Decomposition of tetramethylammonium cations overlapping with decomposition of oxalate ligand complicates analysis of TGA and DTG curves of (**1**) in the region 200–400 °C. One the other hand, the cluster $K_6[Mo^{V}_4O_4S_4(C_2O_4)_5]$ is stable up to 300 °C, following by decomposition of oxalate ligands up to 350 °C. Then, in the case of both complexes, a slow decomposition of binuclear fragments occurs up to 800 °C.

Reactivity of (1) and (2) with Pyrazole and Triazole

As mentioned above, the literature mainly describes coordination to binuclear clusters of carboxylic acids, amino acids and EDTA derivatives. Several works have also been published on the coordination of N-donor heterocycles [20–23]. Despite the different starting compounds used for the synthesis of cluster compounds with organic ligands, the main method of synthesis is the solution method (aqueous solution or organic solvent). In this work, nitrogen heterocycles have been chosen as organic ligands, namely pyrazole and 1,2,4-triazole, which can act on the one hand as terminal ligands, and on the other hand, due to their acid-base properties and the presence of two nitrogen atoms in adjacent positions, as bridging ligands connecting binuclear fragments.

First, the interaction of (**1**) and (**2**) with pyrazole and triazole in aqueous solution was studied by adding organic ligands both during the synthesis of the initial complexes and by performing a direct reaction. At the same time, the ratio of reagents, temperature and reaction time were varied. Crystallization of the reaction products from aqueous solutions resulted in the formation of either crystals of the initial compounds or amorphous products of variable composition. In one of the cases, after the addition

of pyrazole during the synthesis of **(1)**, the new complex $(pzH_2)_2[Mo^V{}_2O_2(\mu - S)_2(\eta^2 - C_2O_4)_2(H_2O)_2]\cdot 3H_2O$ (compound **(3)**) (Fig. 3) was precipitated, which crystals suitable for SCXRD, were obtained from the mother liquor (powder pattern of precipitate is in a good agreement with theoretical one for the structure, Fig. S12). In this case, pyrazole does not act as a ligand, but forms a pyrazolium cation under acidic conditions, which crystallizes with a binuclear cluster anion previously described in the literature in the salts with cesium and sodium cations [33, 36, 37].

Since the coordination of pyrazole and triazole was not achieved, we switched to other conditions for the reaction of **(1)** and **(2)** with organic compounds, namely the reaction in a melt of an organic ligand at high temperatures. In this case, pyrazole and triazole act as both reaction medium and ligand. In addition, the absence of other coordinating solvents (including influence of pH of solution), and higher temperatures may favor the formation of new compounds.

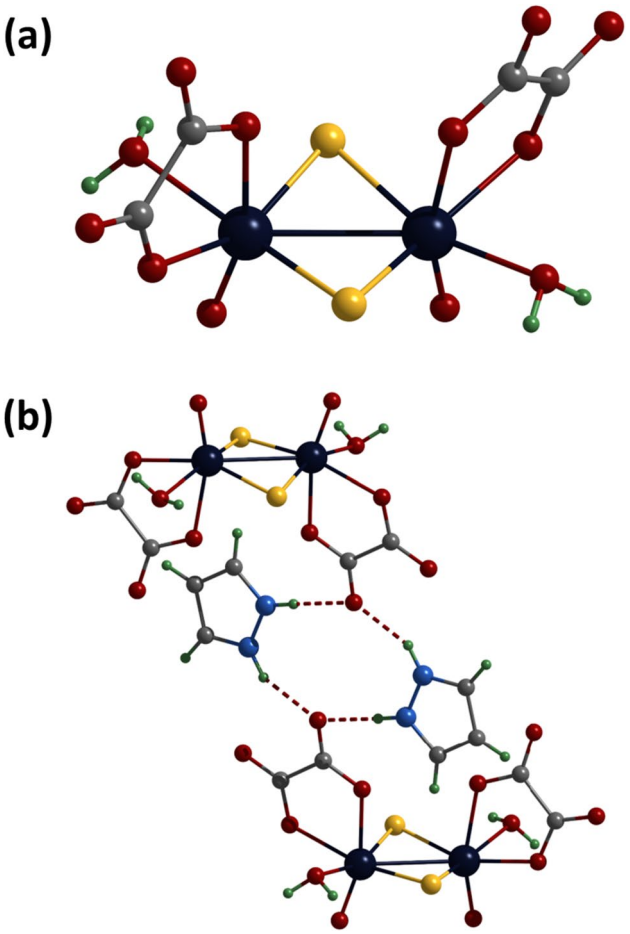

Fig. 3 Structure of cluster anion $[Mo^V{}_2O_2S_2(C_2O_4)_2(H_2O)_2]^{2-}$ (**a**) and hydrogen bonds between cluster anions and pyrazolium cations (**b**) in crystal structure of compound **(3)**. Color code: Mo—dark blue, S—yellow, O—red, C—gray, H—green, N–H···O—dashed red (Color figure online)

Thus, when **(1)** is reacted with pyrazole at 140 °C in a sealed glass ampoule under ambient conditions and the reaction mixture is then cooled slowly over 24 h, crystals of the compound $(Me_4N)_2[Mo^V{}_6O_6S_6(pz)_6(Mo^{VI}O_4)]\cdot 2pzH$ (denoted as **(4a)** phase crystallizing in the orthorhombic space group *P*nma $a = 33.804$ Å, $b = 13.109$ Å, $c = 12.744$ Å, $V = 5674.9$ Å^3) suitable for SCXRD were formed. This compound consists of three $\{Mo^V{}_2O_2S_2\}^{2+}$ units linked in a ring by six bridging pyrazolate ligands and with the molybdate anion $Mo^{VI}O_4{}^{2-}$ serving as a guest "ligand" ($[(Mo^V{}_2O_2(\mu - S)_2)_3(\mu - pz)_6(\mu_6 - Mo^{VI}O_4)]^{2-}$) (Fig. 4a).

The molybdate anion is apparently formed during the partial destruction of the initial complex and its oxidation by atmospheric oxygen. The literature contains mainly examples of binding of binuclear fragments of $\{Mo^V{}_2O_2S_2\}^{2+}$ by bridging hydroxo ligands [3, 33, 38, 39]. Binding of $\{Mo^V{}_2O_4\}^{2+}$ clusters via methylate, phosphate, sulfate and other anions has also been reported [2, 31, 40, 41]. The inner cavity of cyclic compounds based on binuclear fragments $\{Mo^V{}_2O_2Q_2\}^{2+}$ (Q = O, S) may contain phosphate [2, 42] or metalate [3] anions in addition to the carboxylic acids described above. Thus, despite some similar examples of self-assembly of binuclear $\{Mo^V{}_2O_2S_2\}^{2+}$ fragments, compound **(4)** is the first example of a cyclic oxothiomolybdate in which binuclear clusters are linked by bridging organic ligands. On the other hand, in reactions with triazole, we have not been able to isolate individual products or crystallize new compounds. We suspect that similar cyclic compounds may be formed under these conditions, but there is no confirmation at this time.

In the structure of compound **(4a)**, in addition to the anionic complex $[Mo^V{}_6O_6S_6(pz)_6(Mo^{VI}O_4)]^{2-}$, there are two tetramethylammonium cations and two co-crystallizing pyrazole molecules. In the complex anion, the Mo–O fragment of the molybdate anion is disordered over two positions (occupancy of positions 0.3 and 0.7) due to the rotation of the vertex of the MoO_4 tetrahedron down or up relative to the cyclic molecule. Cluster anions are tightly packed in the structure and interact only with neighboring tetramethylammonium cations (weak O···H–C–N hydrogen bonds) (Fig. 4b). When analyzing the distances in the complex, the most significant difference with the literature data is observed in the increase of the Mo-Mo bond length (2.850–2.875 vs 2.804–2.819 Å in **(1)**) in binuclear clusters (Table S2), which may be the reason for adapting the structure to form such a small cycle. The Mo-N bond length (2.188–2.204) is shorter than for coordinated N-donor ligands, but is typical for coordinated bridging pyrazolate ligands (Table S2). The MoO_4 tetrahedron inside the ring is distorted: the Mo–O distances in the ring plane are significantly longer than the Mo–O distances perpendicular to the ring (1.809–1.831 Å and 1.648–1.696 Å, respectively).

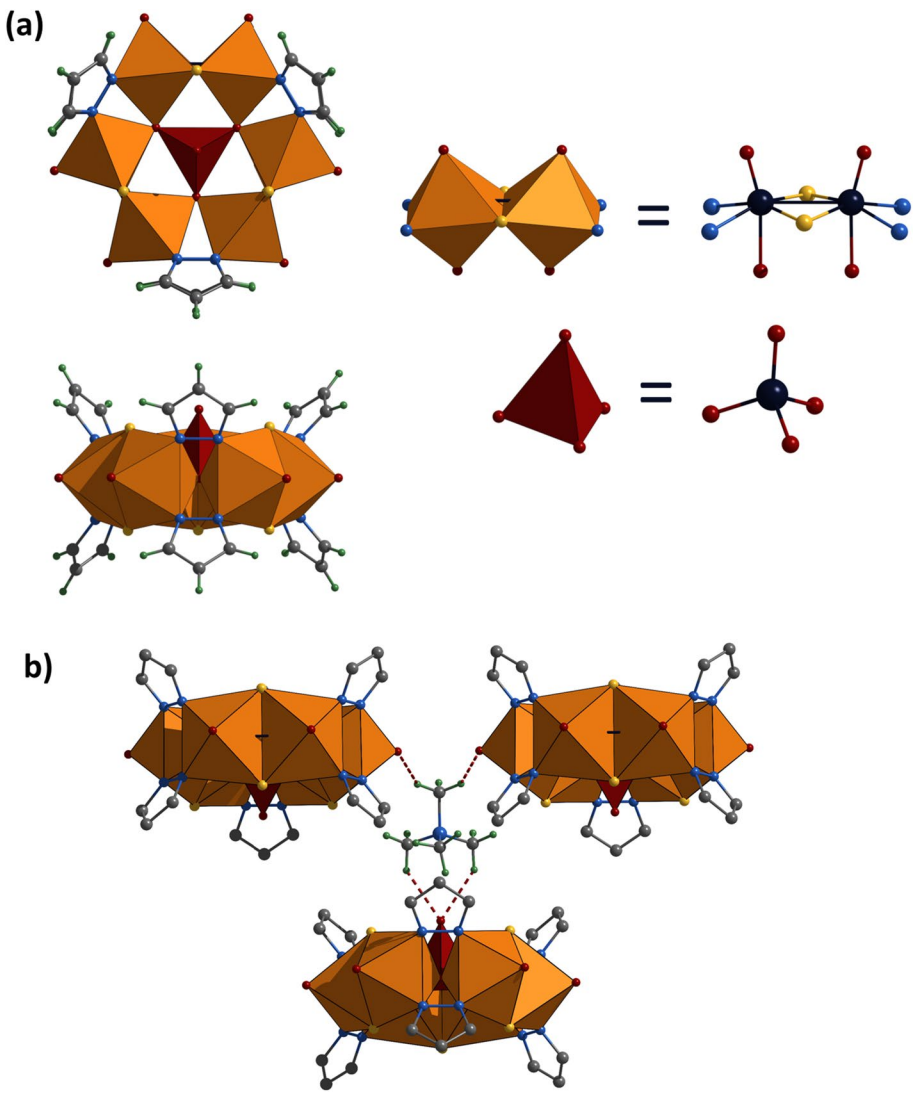

Fig. 4 Structure of cluster anion $[Mo^{V}_{6}O_6S_6(pz)_6(Mo^{VI}O_4)]^{2-}$ (**a**) and packing of cluster anions and tetramethylammonium cations (**b**) in crystal structure of compound **(4a)**. Color code: Mo—dark blue, O—red, S—yellow, C—gray, H—green, $Mo^{V}_{2}N_4O_4S_2$—orange edge-connected octahedrons, $Mo^{VI}O_4$—red tetrahedron, C–H···O—dashed red (Color figure online)

Varying the reaction temperature from 80 to 150 °C showed that no crystalline products were found below 120 °C. One the other hand, varying the reaction time at 140 °C showed the formation of other crystals, the analysis of which by SCXRD reveals the presence of the same anion $[Mo^{V}_{6}O_6S_6(pz)_6(Mo^{VI}O_4)]^{2-}$ (denoted as **(4b)** phase: $P2_1$ a = 16.6196(3) Å, b = 15.3448(3) Å, c = 21.7308(4) Å, β = 98.992(1)°, V = 5473.8(2) Å^3) and **(4c)** phase: $P2_1/n$ a = 21.916(2) Å, b = 20.062(1) Å, c = 22.491(2) Å, β = 91.257(3)°, V = 9886.2(1) Å^3). However, the quality of the crystals was not sufficient enough to determine the cations and the exact solvate composition. Powder X-ray diffraction analysis of the reaction mixtures showed that the reflections of **(4b)** and **(4c)** phases begin to appear after 3 h of heating (Fig. S13). After 9 h, the reflections of **(4a)** phase are clearly visible. After 48 h, the mixture of **(4a)** and **(4b)** phase reflections were found. It is likely that the presence of a mixture of products is due to the different cationic and solvate composition of $K_x(NMe_4)_{2-x}[Mo^{V}_{6}O_6S_6(pz)_6(Mo^{VI}O_4)]\cdot$(Solvate), since the starting compound **(1)** contains a mixed cation.

Despite the optimized conditions for obtaining the crystalline phase, we were not able to isolate compound **(4)** in pure form. The complex is insoluble in water and in many organic solvents except DMSO and DMF. The structure of the complex in DMSO solution was determined by ^{1}H NMR spectroscopy. In addition to the signals of the solvated pyrazole molecules (6.24 and 7.58 for the signals of the protons in the 4 and 3 or 5 positions of the ring), the spectrum contains a group of signals of the coordinated pyrazole ligands: two doublets at 8.36 and 8.27 ppm, two triplets at 6.60 and 6.59 ppm with an integral intensity ratio of 6:6:3:3, as well as other signals of lower intensity (integrated intensity is 6 times smaller than the main signals) (Fig. S14). Thus, during the coordination of the pyrazolate ligands, a downfield shift of all signals of the

ligand protons is observed, and the signals of the protons in positions 3 and 5 have a stronger shift since they are closer to the coordination centers. Due to the presence of the molybdate anion in the center of the cyclic molecule, the signals of the protons of the ligands on opposite sides of the ring plane become non-equivalent, which is expressed in two doublets and triplets. Signals of lower intensity may be due to impurity complexes of different nuclearity or to the complexes in which the molybdate anion in absent.

The reaction of compound **(2)** with a melt of pyrazole or triazole leads to the formation of crystals of the binuclear cluster complexes $K_2[Mo^V_2O_2S_2(C_2O_4)_2(pzH)_2]\cdot 0.5pzH\cdot 1.4H_2O$ (denoted as **(5)**) and $K_{1.5}H_{0.5}[Mo^V_2O_2S_2(C_2O_4)_2(trzH)_2]\cdot 2trzH\cdot H_2O$ (denoted as **(6)**), which are suitable for SCXRD. The reaction proceeds with high yields of about 70% within 6 h at 140 °C. Longer heating of the reaction mixture or higher temperatures lead to decomposition of the cluster complexes with formation of black or brown amorphous compounds of unknown composition. Excess of organic ligand and by-products were removed by repeated washing of crystals of **(5)** and **(6)** with a mixture of ethanol and water. According to the PXRD data, the diffraction patterns of the crystalline compounds are in good agreement with the theoretical ones obtained from the SCXRD data (Figs. S15, S16).

During the reaction, the bridging oxalate ligand in **(2)** is substituted by two organic ligands (the triazole is coordinated by a nitrogen atom in the fourth position) to form the anion $[Mo^V_2O_2(\mu - S)_2(\eta^2 - C_2O_4)_2L_2]^{2-}$ (Fig. 5 and 6). In addition to the cluster anion, structures **(5)** and **(6)** contain potassium cations, solvate molecules of water and pyrazole/triazole. In compound **(6)**, only 1.5 potassium cations per cluster anion were found, and the remaining charge, we assume, is compensated by a proton, which can be localized on solvate molecules of water and triazole.

The structure of compound **(5)** contains three structurally independent cluster anions. The first anion forms infinite chains along the *b* axis by hydrogen bonds N–H···O (N···O distances of 2.765–2.807 Å) between the pyrazole and oxalate ligands (Fig. 5b). The second anion forms infinite layers along the *ab* plane by K···O contacts between potassium cations and oxalate ligands (distances of 2.714–2.850 Å) (Fig. 5c). The third anion is also linked to this layer by potassium cations (K···O distances of 2.692–2.853 Å) (Fig. S17). These potassium cations also link layers and chains by K···O contacts (distances of 2.731–2.814 Å) (Fig. S17), forming a densely packed complex structure. Solvate molecules of

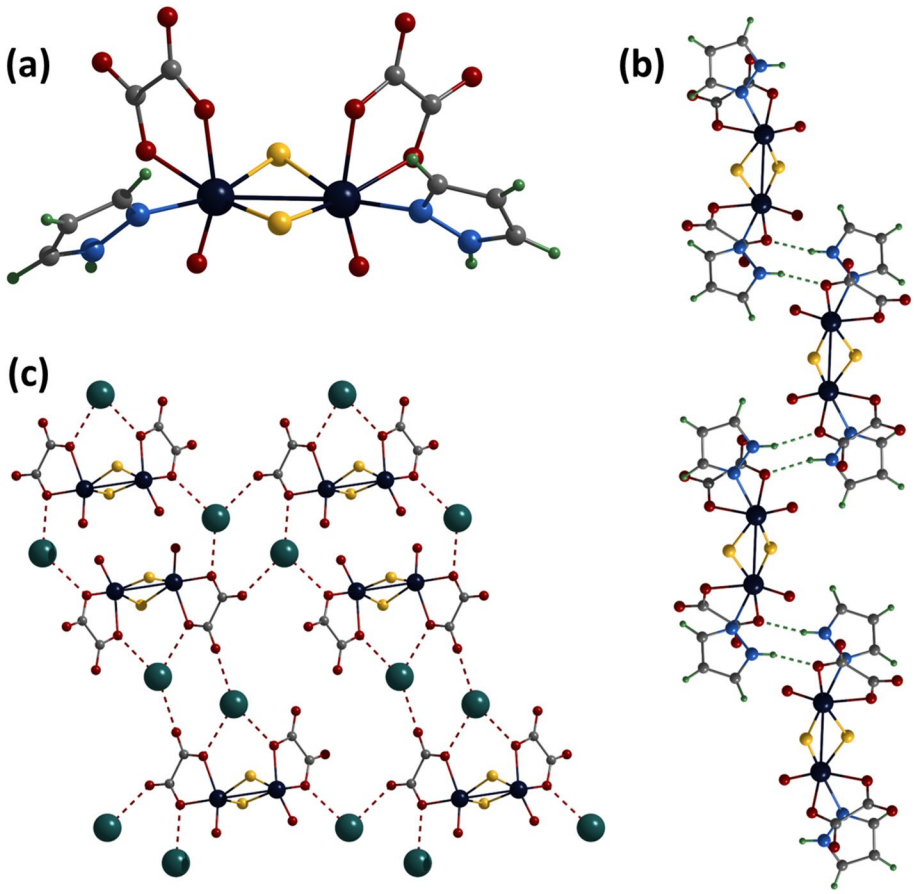

Fig. 5 Structure of cluster anions $[Mo^V_2O_2S_2(C_2O_4)_2(pzH)_2]^{2-}$ (**a**) and packing of cluster anions forming chains (**b**) or layers (**c**) in the crystal structure of compound **(5)**. Color code: Mo—dark blue, S—yellow, O—red, C—gray, H—green, N–H···O—dashed green, K···O—dashed red (Color figure online)

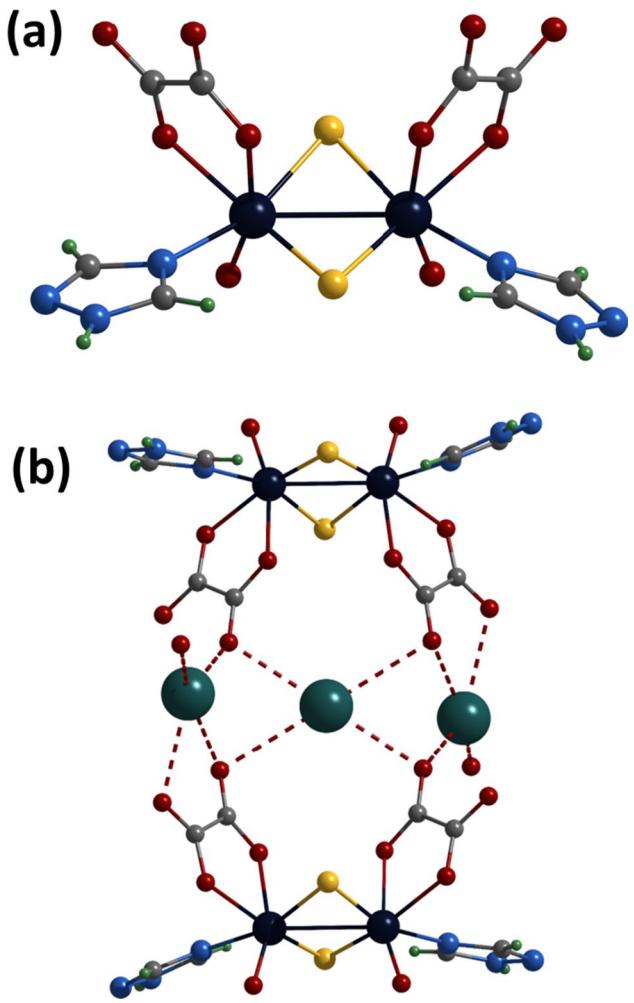

Fig. 6 Structure of cluster anions $[Mo^{V}_2O_2S_2(C_2O_4)_2(trzH)_2]^{2-}$ (**a**) and interactions between of cluster anions and potassium cations (**b**) in the crystal structure of compound (**6**). Color code: Mo—dark blue, S—yellow, O—red, C—gray, H—green, K—dark cyan, K···O—dashed red (Color figure online)

water or pyrazole complement the potassium coordination spheres.

In the structure of compound (**6**), two cluster anions are linked by the contacts between potassium cations and oxygen of oxalate ligands (K···O distances of 2.746–3.083 Å) (Fig. 6b, Fig. S18). Also, potassium cation interacts with solvate triazole (K···N distances of 2.731–2.956 Å) and water (K···O distances of 3.071 Å) molecules. Such fragments are connected to each other in endless chains along the *a* axis by hydrogen bonds between solvate water molecules and oxalate ligands of the neighboring fragment (O···O distances of 2.770 Å), as well as by π–π stacking interactions (distances between centers of 3.701 Å) between solvate triazole molecules. The chains are linked by N–H···O hydrogen bonds (N···O distances of 2.709 Å) between coordinated triazole ligands and oxalate ligands of the adjacent chain (Fig. S19).

The ^{1}H NMR spectra of compounds (**5**) and (**6**), both in D_2O and DMSO-d_6, contain only signals from the protons of the organic ligand, which are practically not shifted with respect to the free ligand and have the same symmetrical pattern, as for example the equivalence of the protons in the 3 and 5 positions of pyrazole. Based on these data, we assume that the complexes dissociate in solution, which may have been the reason for the impossibility of their formation in solution methods of synthesis.

Thus, the obtained examples of compounds with pyrazole and triazole demonstrate the importance of the structure of the starting oxothiomolybdate complex. By introducing the cyclic compound $[Mo^{V}_8O_8S_8(OH)_8(C_2O_4)]^{2-}$ into the reaction in melt of ligand, a cyclic complex $[Mo^{V}_6O_6S_6(pz)_6(Mo^{VI}O_4)]^{2-}$ was obtained. A similar situation is observed in the reaction of $[Mo^{V}_4O_4S_4(C_2O_4)_5]^{6-}$ with organic ligands with preservation of the binuclear clusters, only in this case the clusters are no longer connected to each other by bridging oxalate. Regardless of the reaction conditions, we did not observe any transitions of complexes with cyclic structure into binuclear ones and vice versa.

Conclusion

In summary, in this work the synthesis of the cyclic anionic complex $[Mo^{V}_8O_8S_8(OH)_8(C_2O_4)]^{2-}$, as well as the oxothiomolybdate $[Mo^{V}_4O_4S_4(C_2O_4)_5]^{6-}$ in which two binuclear clusters are connected by a bridging oxalate anion, was optimized. The reactions of these complexes with pyrazole and 1,2,4-triazole were then studied both in solution and in melts of organic ligands. Thus, the addition of organic ligands during the synthesis of the starting compounds does not lead to the coordination of pyrazole or triazole, and only in one case it was possible to obtain a compound where pyrazole acts as a pyrazolium cation for the cluster anion $[Mo^{V}_2O_2S_2(C_2O_4)_2(H_2O)_2]^{2-}$. The most interesting results were obtained in reactions in the melt of the ligands, where the reaction product depends on the structure of the starting complex: (i) preservation of the cyclic structure (but with a decrease in nuclearity) with coordination of pyrazole as bridging ligand in the case of the new oxothiomolybdate $[Mo^{V}_6O_6S_6(pz)_6(Mo^{VI}O_4)]^{2-}$; (ii) replacement of the bridging oxalate ligand by an organic one with formation of anionic binuclear clusters $[Mo^{V}_2O_2S_2(C_2O_4)_2L_2]^{2--}$. This work demonstrates new fundamental approaches to extending the chemistry of oxothiomolybdates: (i) carrying out reactions in melts of organic compounds; (ii) using heterocyclic compounds of the azole series to link binuclear clusters. The

results obtained will serve as a basis for the development of oxothiomolybdates to obtain new materials.

Supplementary Information The online version contains supplementary material available at https://doi.org/10.1007/s10876-024-02595-z.

Acknowledgments This work was supported by the Russian Science Foundation (No. 22-23-00660). The authors thank the Ministry of Science and Higher Education of the Russian Federation. The authors thank XRD Facility of NIIC SB RAS and personally thank to Sukhikh A.S. and Yudin V.N. for the data collection.

Author Contributions Formal analysis: AVK, NVK; Investigation: AVK, NVK; Validation: AVK, DVE; Conceptualization: DVE, AAI; Visualization: DVE, AAI; Data curation: DVE, AAI; Funding acquisition: AAI; Project administration: AAI; Supervision: AAI; Writing—original draft: DVE, AAI; Writing—review and editing: MAS.

Funding This work was supported by the Russian Science Foundation (No. 22-23-00660).

Data Availability Crystal structure data can be obtained free of charge from The Cambridge Crystallographic Data Centre via www.ccdc.cam.ac.uk/data_request/cif or are available on request from the corresponding author.

Declarations

Conflict of interest There are no conflicts to declare.

Ethical Approval Not applicable.

References

1. A. Elliott and H. N. Miras (2022). *J. Coord. Chem.* **75**, 1467. https://doi.org/10.1080/00958972.2022.2086049.
2. E. Cadot, A. Dolbecq, B. Salignac, and F. Sécheresse (1999). *Chem. Eur. J.* **5**, 2396.
3. A. Dolbecq, E. Cadot, and F. Sécheresse (1998). *Chem Commun*. https://doi.org/10.1039/A805453C.
4. B. Salignac, S. Riedel, A. Dolbecq, F. Sécheresse, and E. Cadot (2000). *J. Am. Chem. Soc.* **122**, 10381. https://doi.org/10.1021/ja001878t.
5. Q.-Y. Xu, Z. Xin, M.-J. Hu, H.-T. Shi, A.-Q. Jia, and Q.-F. Zhang (2023). *J. Clust. Sci.* **34**, 285. https://doi.org/10.1007/s10876-022-02219-4.
6. E. Cadot and F. Sécheresse (2002). *Chem Commun*. https://doi.org/10.1039/B203497M.
7. A. Hijazi, J. C. Kemmegne-Mbouguen, S. Floquet, J. Marrot, C. R. Mayer, V. Artero, and E. Cadot (2011). *Inorg. Chem.* **50**, 9031. https://doi.org/10.1021/ic201239y.
8. B. Keita, S. Floquet, J.-F. Lemonnier, E. Cadot, A. Kachmar, M. Bénard, M.-M. Rohmer, and L. Nadjo (2008). *J. Phys. Chem. C* **112**, 1109. https://doi.org/10.1021/jp0774138.
9. A. Fuior, A. Hijazi, O. Garbuz, V. Bulimaga, L. Zosim, D. Cebotari, M. Haouas, I. Toderaş, A. Gulea, and S. Floquet (2022). *J. Inorg. Biochem.* **226**. https://doi.org/10.1016/j.jinorgbio.2021.111627.
10. B. Spivack and Z. Dori (1975). *J Chem Soc Dalton Trans*. https://doi.org/10.1039/DT9750001077.
11. J.-F. Wu, D.-M. Li, L.-F. Cui, C.-F. Zhuang, S.-N. Song, T.-G. Wang, J.-Q. Xu, H.-Q. Jia, and N.-H. Hu (2007). *Appl. Organomet. Chem.* **21**, 1033. https://doi.org/10.1002/aoc.1327.
12. Y.-H. Xing, J.-Q. Xu, D.-M. Li, H.-R. Sun, W.-M. Bu, L. Ye, G.-D. Yang, and Y.-G. Fan (1998). *Synth. React. Inorg. Metar.* **28**, 1493. https://doi.org/10.1080/00945719809351692.
13. R. Yoshida, S. Ogasahara, H. Akashi, and T. Shibahara (2012). *Inorg. Chim. Acta* **383**, 157. https://doi.org/10.1016/j.ica.2011.10.070.
14. T. Shibahara, S. Ogasahara, and G. Sakane (2008). *Acta Cryst.* **E64**. https://doi.org/10.1107/S1600536808007757.
15. S. Duval, S. Floquet, C. Simonnet-Jégat, J. Marrot, R. N. Biboum, B. Keita, L. Nadjo, M. Haouas, F. Taulelle, and E. Cadot (2010). *J. Am. Chem. Soc.* **132**, 2069. https://doi.org/10.1021/ja909762p.
16. A. Kojima, S. I. Ooi, Y. Sasaki, K. Z. Suzuki, K. Saito, and H. Kuroya (1981). *Bull. Chem. Soc. Jap.* **54**, 2457. https://doi.org/10.1246/bcsj.54.2457.
17. B. Spivack and Z. Dori (1973). *J Chem Soc Dalton Trans*. https://doi.org/10.1039/DT9730001173.
18. D. Cebotari, S. Calancea, J. Marrot, R. Guillot, C. Falaise, V. Guérineau, D. Touboul, M. Haouas, A. Gulea, and S. Floquet (2023). *Dalton Trans.* **52**, 3059. https://doi.org/10.1039/D2DT03760B.
19. A. Fuior, D. Cebotari, O. Garbuz, S. Calancea, A. Gulea, and S. Floquet (2023). *Inorg. Chim. Acta* **548**. https://doi.org/10.1016/j.ica.2022.121372.
20. M. Cindrić, V. Vrdoljak, B. Prugovečki, and B. Kamenar (1998). *Polyhedron* **17**, 3321. https://doi.org/10.1016/S0277-5387(98)00111-9.
21. A. L. Gushchin, Y. L. Laricheva, N. I. Alferova, A. V. Virovets, and M. N. Sokolov (2013). *J. Struct. Chem.* **54**, 752. https://doi.org/10.1134/S0022476613040148.
22. J. Hai-Ying, H. Ryoichi, Y. Mikio, U. Keisuke, T. Kiyoshi, and S. Yoichi (2005). *Bull. Chem. Soc. Jpn.* **78**, 2161. https://doi.org/10.1246/bcsj.78.2161.
23. J. Mizutani, H. Imoto, and T. Saito (1997). *Acta Cryst.* **C53**, 47. https://doi.org/10.1107/S0108270196010116.
24. F. Celik, Y. Unver, B. Barut, A. Ozel, and K. Sancak (2018). *Med. Chem.* **14**, 230. https://doi.org/10.2174/1573406413666171120165226.
25. M. J. Naim, O. Alam, F. Nawaz, M. J. Alam, and P. Alam (2016). *J. Pharm. Bioallied. Sci.* **8**, 2. https://doi.org/10.4103/0975-7406.171694.
26. E. Cadot, B. Salignac, S. Halut, and F. Sécheresse (1998). *Angew. Chem. Int. Ed.* **37**, 611.
27. E. Cadot, B. Salignac, J. Marrot, A. Dolbecq, and F. Sécheresse (2000). *Chem Commun*. https://doi.org/10.1039/A909024J.
28. G. M. Sheldrick (2015). *Acta Cryst.* **A71**, 3. https://doi.org/10.1107/S2053273314026370.
29. G. M. Sheldrick (2015). *Acta Cryst.* **C71**, 3. https://doi.org/10.1107/S2053229614024218.
30. C. du Peloux, A. Dolbecq, E. Cadot, J. Marrot, and F. Sécheresse (2003). *J. Mol. Struct.* **656**, 37. https://doi.org/10.1016/S0022-2860(03)00332-6.
31. B. Modec, J. V. Brenčič, and J. Koller (2004). *Eur. J. Inorg. Chem.* **2004**, 1611. https://doi.org/10.1002/ejic.200300741.
32. S. Takashi, O. Shunichiro, and K. Hisao (1982). *Bull. Chem. Soc. Jap.* **55**, 3742. https://doi.org/10.1246/bcsj.55.3742.
33. A. Dolbecq, B. Salignac, E. Cadot, and F. Secheresse (1998). *Bull. Pol. Acad. Sci.* **46**, 237.
34. K. Mennemann and R. Mattes (1979). *J. Chem. Res.* **100**, 1343.
35. B. Kamenar, B. Kaitner, and N. Strukan (1992). *Bull. Slovenian Chem. Soc.* **39**, 357.
36. W. S. McDonald (1978). *Acta Cryst.* **B34**, 2850. https://doi.org/10.1107/S0567740878009371.
37. B. Kamenar, B. Kaitner, and N. Strukan (1991). *Croat. Chem. Acta* **64**, 329.
38. A. Hijazi, J. C. Kemmegne-Mbouguen, S. Floquet, J. Marrot, J. Fize, V. Artero, O. David, E. Magnier, B. Pégot, and E. Cadot

(2013). *Dalton Trans.* **42**, 4848. https://doi.org/10.1039/C2DT32447D.
39. H.-Y. Zang, A. R. de la Oliva, H. N. Miras, D.-L. Long, R. T. McBurney, and L. Cronin (2014). *Nat. Commun.* **5**, 3715. https://doi.org/10.1038/ncomms4715.
40. C. du Peloux, A. Dolbecq, P. Mialane, J. Marrot, and F. Sécheresse (2004). *Dalton Trans*. https://doi.org/10.1039/B401250J.
41. S.-Y. Wang, X. Dong, and Z.-H. Zhou (2021). *J. Solid State Chem.* **300**. https://doi.org/10.1016/j.jssc.2021.122229.
42. R. C. Haushalter and F. W. Lai (1989). *Inorg. Chem.* **28**, 2904. https://doi.org/10.1021/ic00314a004.